



A novel coating based on carbon nanotubes/poly-*ortho*-phenylenediamine composite for headspace solid-phase microextraction of polycyclic aromatic hydrocarbons

M. Behzadi^{a,b}, E. Noroozian^a, M. Mirzaei^{a,*}

^a Department of Chemistry, Shahid Bahonar University of Kerman, P.O. Box 76169-133, Kerman, Iran

^b Young Research Society, Shahid Bahonar University of Kerman, Kerman, Iran

ARTICLE INFO

Article history:

Received 8 January 2013

Received in revised form

14 February 2013

Accepted 15 February 2013

Available online 4 March 2013

Keywords:

Solid-phase microextraction

Gas chromatography

Poly-*o*-phenylenediamine

Carbon nanotubes

Polycyclic aromatic hydrocarbons

ABSTRACT

A novel nanocomposite coating made of poly-*o*-phenylenediamine (PoPD) and oxidized multiwalled carbon nanotubes (MWCNTs) was electrochemically prepared for the first time on stainless steel wire. Subsequently, it was applied to headspace solid-phase microextraction (HS-SPME) and gas chromatographic analysis of biphenyl and seven polycyclic aromatic hydrocarbons (PAHs). The effects of polymerization potential, polymerization time, concentration of *o*-phenylenediamine and oxidized MWCNTs were investigated on the coating process. The fiber coating was carried out easily and in a reproducible manner, and the produced fiber was stable at high temperatures. The surface morphology of the coating was examined by scanning electron microscopy (SEM). The effects of various parameters on the efficiency of HS-SPME process, such as desorption temperature, desorption time, extraction temperature, extraction time and ionic strength were also studied. Under optimized conditions, the calibration graphs were linear in the range of 0.1–300 ng mL⁻¹, and the detection limits for biphenyl and PAHs studied were between 0.02 and 0.09 ng mL⁻¹. The intra-day and inter-day relative standard deviations obtained at 5 ng mL⁻¹ concentration level ($n=5$), using a single fiber, were 3.2–7.8% and 5.2–9.3%, respectively. The fiber-to-fiber RSD% ($n=3$) were 6.2–11.3% at 5 ng mL⁻¹. The proposed HS-SPME method was successfully applied for the analysis of PAHs in water samples.

© 2013 Elsevier B.V. All rights reserved.

1. Introduction

Polycyclic aromatic hydrocarbons (PAHs) comprise a group of chemicals that were produced during the incomplete burning of fuels, garbage or other organic substances [1]. PAHs can also be found in coal tar, bitumen, crude oil, creosote and roofing tar. Therefore, the distribution of PAHs in the environment is extensive. Since, they were found in soil, air, water, food or household products, the general public may be exposed to PAHs [2–4]. These contaminants are of considerable interest, because some are highly carcinogenic and/or genotoxic in laboratory animals. Some PAHs have been implicated in breast, lung, and colon cancers in humans [5–7]. This is because PAHs bind covalently to DNA, and cause disruptions in its replication. This mechanism, with some modifications, occurs with all carcinogenic PAHs [8]. Therefore, the determination of PAHs in environmental samples is essential.

* Corresponding author. Tel./fax: +98 341 3222033.

E-mail addresses: m_mirzaei@mail.uk.ac.ir,
m_mirzaei36@yahoo.com (M. Mirzaei).

There are several sample preparation techniques for the determination of these contaminants in the environment. These include: liquid–liquid microextraction [9], solid-phase extraction (SPE) [10,11], stir-bar sorptive extraction (SBSE) [12,13], solid-phase microextraction (SPME) [14–17] and hollow-fiber liquid-phase microextraction [18]. SPME is an extremely attractive alternative to classical extraction methods. It combines sampling, extraction and preconcentration of analytes in a single step. This method enables direct desorption of analytes into the chromatographic systems for analysis. SPME can be applied to both headspace and direct sample analysis with excellent sensitivity and good selectivity [19–21]. However, when volatile compounds or very complex samples are analyzed, headspace solid-phase microextraction (HS-SPME) is preferred.

As SPME greatly depends on sorbent chemistry and coating technology, development of new sorbent materials with improved properties is essential.

In recent years, intrinsically conducting polymers with conjugated double bonds have attracted much attention as advanced materials. They can be easily synthesized through chemical or electrochemical means in both aqueous and non-aqueous media. Electrochemical synthesis is more convenient, because the polymer can be deposited directly on the surface of a metal wire with

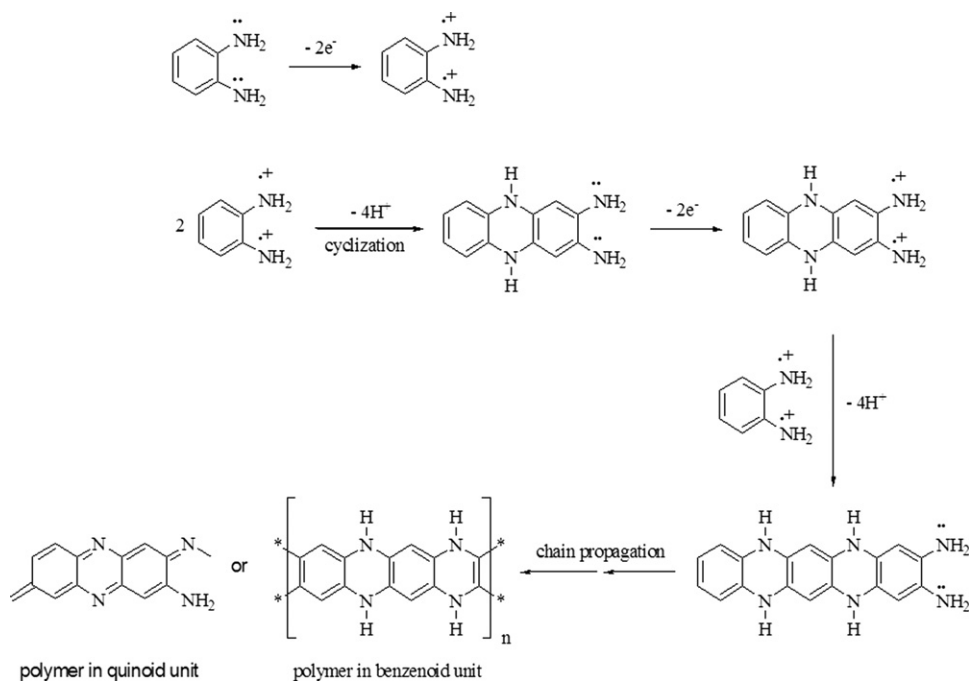
better mechanical strength than silica fibers originally used in SPME [22].

Phenylenediamines belong to a class of aniline derivatives having an extra $-NH_2$ group in *ortho*-, *meta*- or *para*-position. *O*-phenylenediamine (oPD) is the most frequently studied member of the group [23]. Poly-*ortho*-phenylenediamine (PoPD) is a widely used permselective polymer in the construction of biosensors for a range of analytes, such as hydrogen peroxide, ascorbic acid, uric acid, acetaminophen and cysteine [24]. PoPD can be deposited electrochemically from *o*-phenylenediamine solutions at neutral pH to produce a thin self-sealing insulating polymer on the electrode surface [25]. The mechanism shown in Scheme 1 has been proposed for the electrochemical growth of PoPD [26]. The monomer is initially oxidized to give the dication radical, which then undergoes chemical coupling to produce a dimer which could be further oxidized. The dication of the dimer could further undergo polymerization to produce a linear chain polymer. Also it can become cyclized to produce a ladder structure through polymerization of the oxidized products.

When the film grows to reach enough thickness to become an insulator covering the electrode surface, further access of monomers to the electrode surface is prohibited. The thickness of PoPD, generated under these conditions, is typically 10–35 nm [25,27]. This is too thin to absorb an adequate amount of analytes, when used as a sorbent in SPME.

Carbon nanotubes (CNTs) have attracted considerable attention since their discovery by Iijima in 1991 [28]. They have been extensively used in a variety of applications. These applications are based on unusual physical or chemical properties of CNTs, such as their highly accessible surface area, excellent electrical conductivity, high mechanical strength and good chemical stability [29]. It has been shown that the introduction of CNTs into a polymer matrix improves electrical, as well as mechanical properties of the original polymer [30,31].

The self-sealing growth of non-conducting polymers, such as poly-*o*-aminophenol is mitigated by using an aqueous suspension of oxidized CNTs as supporting electrolyte during their preparation [32]. The mechanism behind this approach is that, CNTs serve as anionic charge carriers in the liquid phase during electro-



Scheme 1. The mechanism of electrochemical growth of PoPD.

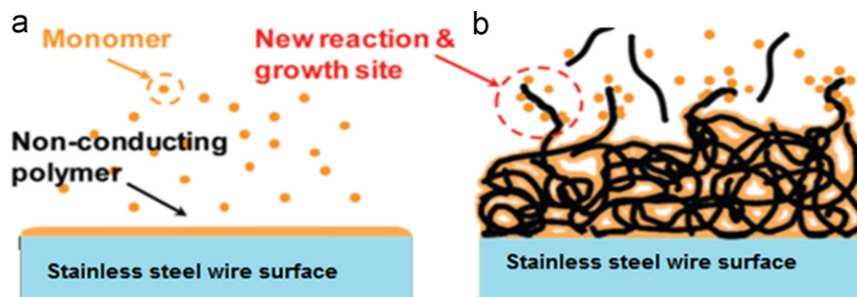


Fig. 1. Schematic diagrams of the steel wire covered with (a) a pure non-conducting polymer layer and (b) a non-conducting polymer/MWCNTs composite layer on which the interconnected MWCNTs represent the electrode sites where further electropolymerization occurs [32].

co-deposition of the composite polymer. CNTs also play the role of backbone of the porous structure within the composite. More importantly, during electro-co-deposition, the dispersed CNTs provide extra electron pathways and new reaction sites for continuous electropolymerization of poly-*o*-aminophenol (Fig. 1) [32].

In the present work, attempts were made to prepare a stainless steel SPME fiber coated with oxidized multiwalled carbon nanotubes/poly-*o*-phenylenediamine composite (MWCNTs/PoPD) through an electrochemical polymerization technique. Then, the extraction capability of the nanocomposite was examined towards PAHs as important environmental pollutants.

2. Experimental

2.1. Chemicals

Naphthalene, acenaphthylene, fluorene, phenanthrene, anthracene, fluoranthene, pyrene and biphenyl were purchased from Fluka (Buchs, Switzerland). HPLC grade acetonitrile and reagent grade sodium chloride were obtained from Merck (Darmstadt, Germany). Individual stock solutions of each PAH (1000 mg L⁻¹) were prepared in acetonitrile. Stock mixture of the target analytes was prepared at a final concentration of 100 mg L⁻¹ in acetonitrile. From this solution, several standard working solutions were prepared in distilled water. All stock and working solutions were stored at 4 °C. *Ortho*-phenylenediamine was obtained from Merck (Darmstadt, Germany). It was recrystallized from hot water before use and stored in a dark bottle under nitrogen atmosphere. Multiwalled carbon nanotubes (Plasma Chem, Berlin, Germany) were 20–40 nm in diameter and 1–10 µm in length. Helium and nitrogen (≥99.999%) were obtained from Sabalan Co. (Tehran, Iran).

2.2. Instruments

The SPME device was home made. It consisted of a 23 gauge, 9.0 cm stainless steel spinal needle purchased from Dr. Japan Co. (Tokyo, Japan) and housed in a 6.0 cm hollow cylinder of Al with two nuts and two pieces of rubber septum. A piece of steel wire (type 302, 17 cm × 0.3 mm) passing through the septum acted as the SPME fiber. One end of the fiber was attached to a cap and 3 cm of the other end was coated with a thin film of MWCNTs/PoPD. All electrochemical measurements were carried out in a conventional three electrodes cell, powered by a Behpajuh potentiostat/galvanostat model BHP 2061-C (Isfahan, Iran). The steel wire used as the working electrode was obtained from American Orthodontics (WI, USA). A Pt counter electrode and a saturated calomel reference electrode (SCE) were from Azar Electrode Co. (Urmieh, Iran). For stirring and heating the samples during the SPME process, a Jenway model 1000 hot plate-stirrer (Bibby Scientific, Manchester, UK) was used. FTIR spectra were recorded by a Tensor 27 FTIR spectrometer from Bruker (Ettlingen, Germany). The scanning electron micrographs of the fiber surface were obtained using Hitachi S4160 (Tokyo, Japan) scanning electron microscope. Sonications were carried out with a Bandelin Sonorex Super ultrasonic bath (Berlin, Germany). All glassware were washed in ultrapure water and dried at 250 °C.

Separation and quantification of PAHs were carried out using a model 16 A gas chromatograph from Shimadzu (Tokyo, Japan) equipped with a split-splitless injector and flame ionization detector (FID). A BP-10 capillary column (25 m × 0.33 mm I.D., 0.5 µm film thickness) was purchased from Shimadzu (Tokyo, Japan). The column temperature was initially kept at 50 °C for 3 min, then increased at 20 °C min⁻¹ to 190 °C, ramped

at 10 °C min⁻¹ to 260 °C and finally kept for 5 min. Injector and detector temperatures were adjusted at 280 °C and 320 °C, respectively. A Shimadzu 17 A/QP5050 GC/MS instrument (Shimadzu, Tokyo, Japan) equipped with quadrupole analyzer and electron impact ion source (EI) was used for the identification of PAHs in real samples. The MS conditions were: mass range 40–350, electron energy 70 eV, GC/MS interface and ion-source temperatures 230 °C.

2.3. MWCNTs modification

The commercial sample of carbon nanotubes is not dispersible in water even by prolonged sonication. Therefore, to achieve good dispersion of carbon nanotubes, the commercial powder was subjected to chemical oxidation with concentrated nitric acid. MWCNTs (~100 mg) were added to 7 mL of the acid in a round bottomed flask and the mixture was refluxed for 3 h in 110 °C. After cooling, the mixture was transferred onto a filter paper (Whatman No. 41) and washed with copious amount of distilled water until neutral. The oxidized carbon nanotubes can be easily dispersed in aqueous solutions due to the presence of hydrophilic functional groups such as –COOH and –OH.

2.4. Preparation of the composite coating

The oxidized MWCNTs described above were ultrasonically dispersed in water for 45 min. Electro-co-deposition of PoPD and MWCNTs was carried out by potentiostatic polymerization of oPD (10 mL, 0.05 M) in an aqueous suspension of oxidized MWCNTs (0.1 wt %) at room temperature. To adhere the coating firmly to the surface of the wire, the wire surface was first roughened by a smooth sand paper and then washed in acetone while sonicating. It was subsequently washed with distilled water. The presence of an electrolyte is necessary for electropolymerization of nonconducting polymers [32]. Here, the partially ionizable carboxylic acid groups, which were created during the modification of MWCNTs, can act as the necessary electrolyte. Therefore, electropolymerization is performed without any other supporting electrolyte. Thermal conditioning of the fiber was carried out by heating the fiber in an oven at 100 °C for 30 min. Then it was heated in the GC injector port for further 1.5 h at 300 °C. In this way, volatile compounds remaining in the fiber are removed and a smooth chromatographic baseline is obtained.

2.5. Headspace sampling

The working solution (10 mL, 0.02 µg mL⁻¹ PAHs) was placed in a 25 mL vial containing 1.5 g NaCl. Then the vial was sealed with a silicone septum and the solid-phase microextraction from the headspace was carried out at 55 °C. After 45 min, the SPME fiber was removed from the vial and immediately inserted into the GC injection port. The analytes were thermally desorbed, separated by the capillary column and finally detected by FID.

3. Results and discussion

3.1. Characterization of MWCNTs/PoPD composite coating

The composition and morphology of the coating were characterized by Fourier transform infrared (FTIR) spectroscopy and scanning electron microscopy (SEM). Fig. 2 displays the FTIR spectra of *o*-phenylenediamine (a), oxidized MWCNTs (b) and MWCNTs/PoPD composite (c).

The FTIR spectrum for *o*-phenylenediamine shows a typical profile with two peaks at 3378 cm⁻¹ and 3364 cm⁻¹ which are

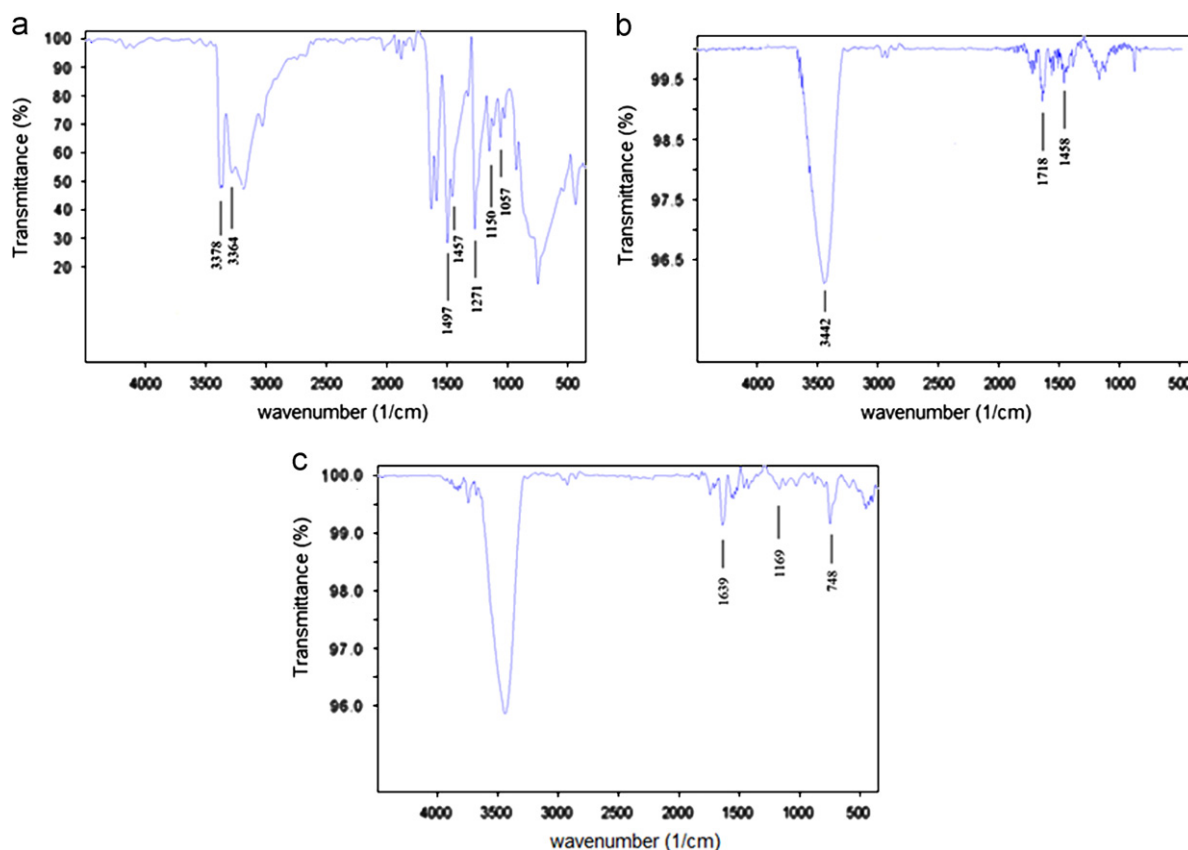


Fig. 2. FTIR spectra of (a) *o*-phenylenediamine, (b) oxidized MWCNTs and (c) MWCNTs/PoPD composite.

due to asymmetrical and symmetrical N–H stretching vibrations. The two peaks at 1457 cm^{-1} and 1497 cm^{-1} are the characteristic bands of the C=C stretching vibrations for benzenoid rings, while the peaks at 1057 cm^{-1} , 1150 cm^{-1} and 1271 cm^{-1} are due to C–N stretching vibrations. It is seen that acid treatment introduces various functional groups on the surface of MWCNTs. The peaks at 1718 cm^{-1} and 1458 cm^{-1} in the spectrum of oxidized MWCNTs can be assigned to C=O stretch and O–H bend, respectively. These functional groups improve the dispersive behavior of oxidized MWCNTs in aqueous solutions. Fig. 2c shows the spectrum of MWCNTs/PoPD. The band at 1639 cm^{-1} is ascribed to the stretching of the C=N bonds. Another two peaks at 1169 cm^{-1} and 748 cm^{-1} might be ascribed to the C–N stretching in the quinoid unit and the C–H out-of-plane bending of aromatic nuclei, respectively.

The SEM studies on the nanocomposite coating revealed that the polymer has a porous and relatively homogeneous structure (Fig. 3).

3.2. Coating optimization

A one-at-a-time strategy was used to optimize various parameters that were affecting the electrochemical coating process. First, the effect of electrical potential on the electrochemical deposition of the coating was studied. This parameter was varied between 0.7 and 1.2 V at 1800 s deposition time. As Fig. 4a shows, the most suitable potential for getting the highest extraction efficiency was found at 1.0 V vs. SCE. To optimize deposition time, electrodeposition was carried out at 1.0 V vs. SCE from an aqueous solution containing 0.1 M oPD and 0.1% (w/v) oxidized MWCNTs. Electrodeposition times were varied between 600 and 2400 s. Fig. 4b shows the extraction efficiency of the fiber increases by increasing

electrodeposition time, but after 1200 s the efficiency generally decreases. Therefore, all further experiments were carried out at 1200 s.

The effect of the concentrations of monomer and oxidized MWCNTs was also investigated. The oPD and MWCNTs concentrations were varied from 0.025 to 0.15 M and 0.025 to 0.3% (w/v), respectively. A constant 1200 s electrodeposition time at 1.0 V vs SCE was used in all cases. The optimum values for oPD and MWCNTs were found to be 0.05 M and 0.10% (w/v), respectively (Fig. 4).

After the coating process in each optimization step, thermal conditioning of the fiber was carried out. Then, the fiber was used for the headspace solid-phase microextraction of PAHs, and the extraction efficiencies were compared.

3.3. SPME optimization

In this section of the work, several variables such as desorption temperature and time, extraction temperature and time, and ionic strength were optimized. It is known that stirring of the sample improves mass transfer in the aqueous phase and induces convection in the headspace SPME. In other words, agitation reduces the time to reach the equilibrium and extraction time by enhancing the diffusion of the analytes towards the fiber. Therefore, efficient stirring of the samples was performed under a maximum but constant rate during all extractions.

3.3.1. Desorption temperature and time

Carry-over is a common problem in SPME analyses. To avoid this effect, the required temperature and time for complete desorption of analytes from the fiber were determined.

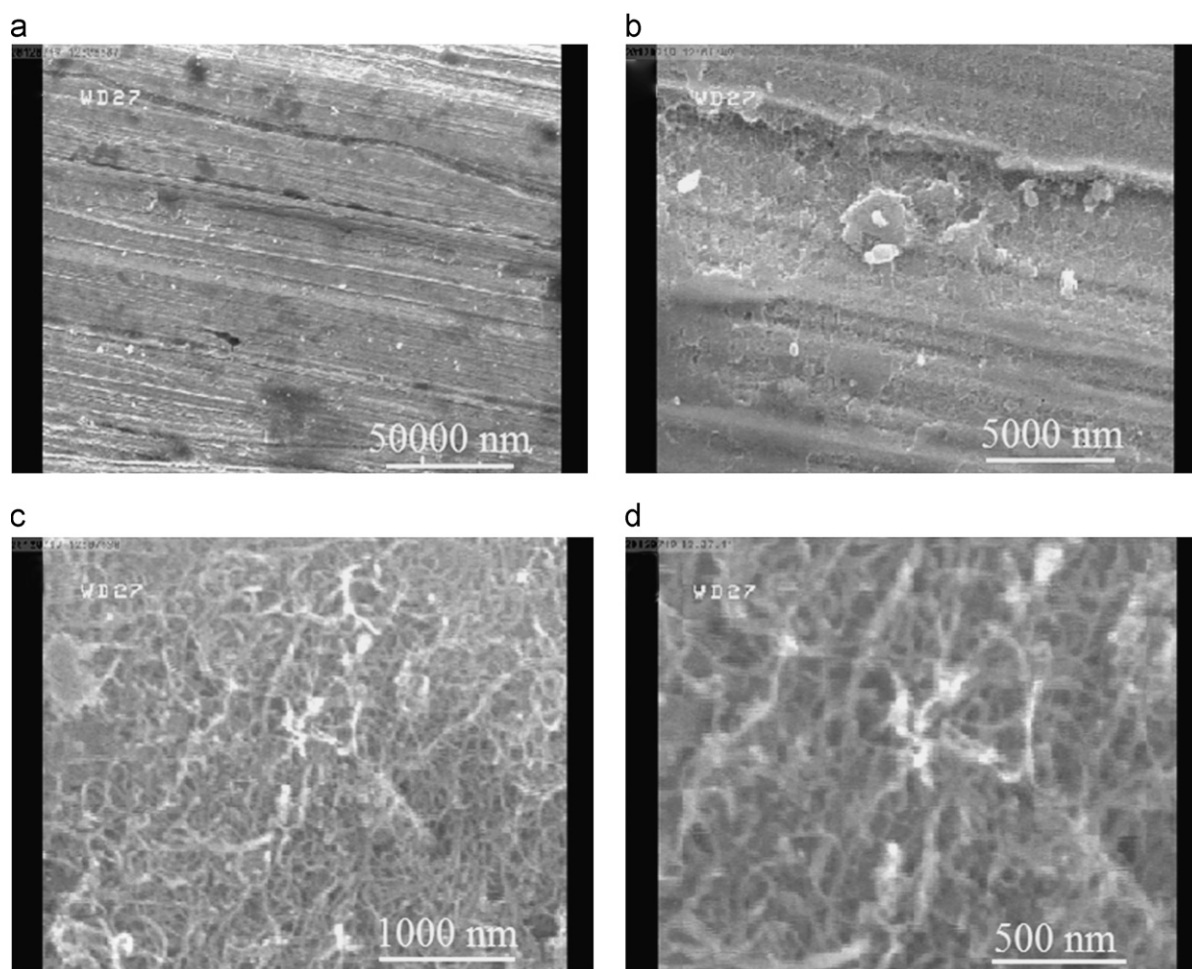


Fig. 3. Scanning electron micrograph images of the surface of MWCNTs/PoPD composite film. (a) Magnification 600 \times , (b) magnification 6000 \times and (c) magnification 30,000 \times and (d) magnification 60,000 \times .

Desorption of the extracted analytes was carried out at temperatures of 170–280 $^{\circ}\text{C}$. Desorption times were also optimized by placing the fiber in the GC injection port for a period of 1–20 min. Based on the results, desorption at 280 $^{\circ}\text{C}$ for 2 min was selected as the optimum values. Under these conditions, maximum desorption occurred and no carry over was observed.

3.3.2. Extraction temperature and time

The sample temperature is an important variable in extraction by HS-SPME. PAHs show a wide range of volatility and the release of those with lower volatility to the headspace during extraction is limited. In general, increasing the temperature could enhance Henry's constants and diffusion coefficients of PAHs. Consequently, the vapor pressure and the concentration of the analytes in the headspace increase. On the other hand, sorption of analytes by the fiber is an exothermic process. Therefore, optimization of the extraction temperature is necessary. This parameter was optimized by exposing the fiber to the sample for 45 min at temperatures ranging from 35 to 75 $^{\circ}\text{C}$. It was observed that, the extraction efficiency for the majority of the compounds increases by increasing the temperature up to 55 $^{\circ}\text{C}$ and then decrease above this temperature (Fig. 5a). However, increasing temperature produces a negative effect on the extraction of some PAHs with higher volatility due to exothermic effect probably [17]. Thus, the extraction temperature was set at 55 $^{\circ}\text{C}$ for all subsequent experiments.

The effect of extraction time on the extraction efficiency was studied by monitoring the peak area as a function of time. Therefore, the fiber was exposed to mixed aqueous solutions of the PAHs at 0.02 $\mu\text{g mL}^{-1}$ each, while the extraction time was varied from 15 to 75 min. Extraction temperature was set at the optimized 55 $^{\circ}\text{C}$ and the analytes were desorbed at 280 $^{\circ}\text{C}$ for a period of 2 min. As Fig. 5b shows, an extraction time of 45 min was sufficient to reach equilibrium.

3.3.3. Ionic strength

It is obvious that, the water solubility of an organic compound is reduced by adding a salt to an aqueous solution of the substance. Thus, the partitioning of analytes from the aqueous solution to the headspace is improved. In this section, the influence of ionic strength was studied by adding different amounts of sodium chloride to aqueous solutions, ranging from 0 to 30% (w/v). As shown in Fig. 5c, at salt concentrations above 15%, the responses for all analytes are nearly constant. Therefore, in subsequent experiments, 15% sodium chloride was added to all sample solutions before extractions.

3.4. Method validation

Figures of merit including, limit of detection (LOD), linear range (LR) and precision in terms of reproducibility and repeatability (RSD %) for the present method are given in Table 1. The

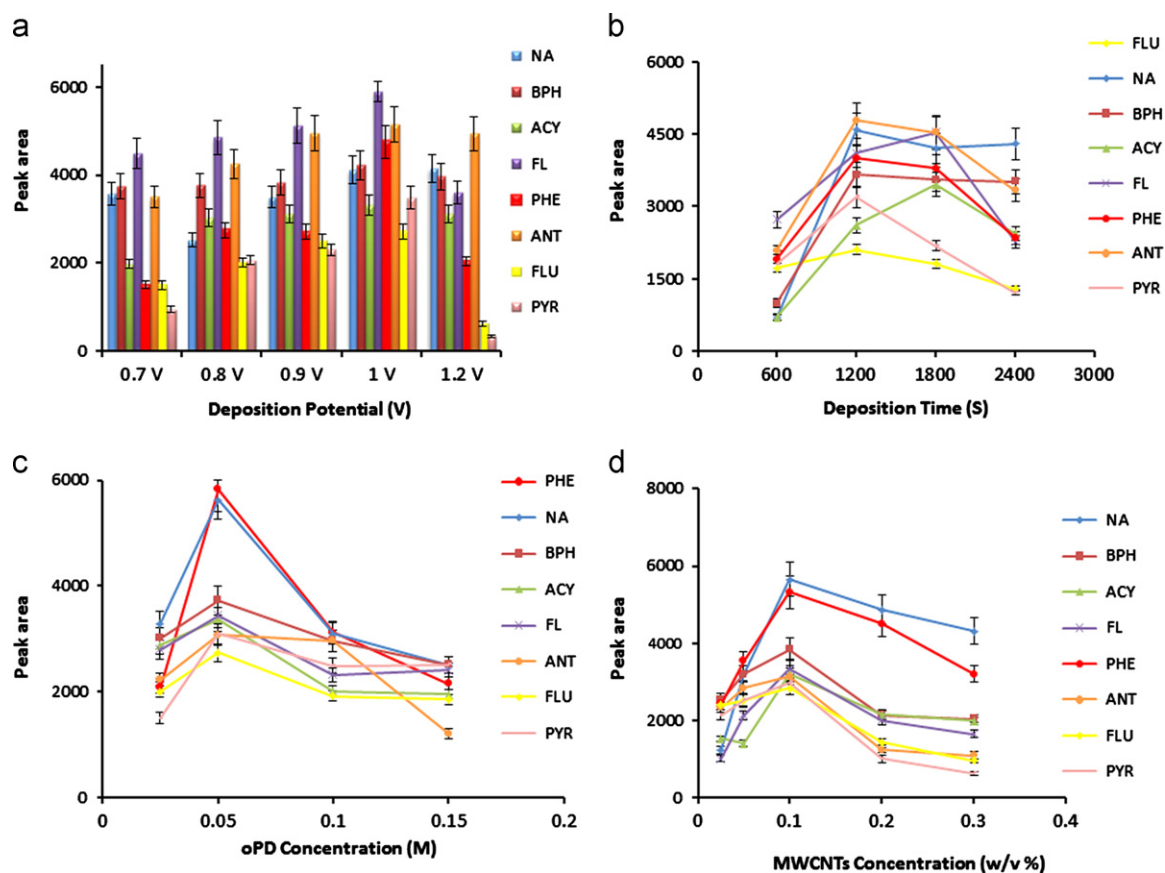


Fig. 4. Effect of coating parameters on the extraction efficiency: (a) deposition potential, (b) deposition time, (c) oPD concentration and (d) MWCNTs concentration; $n=3$.

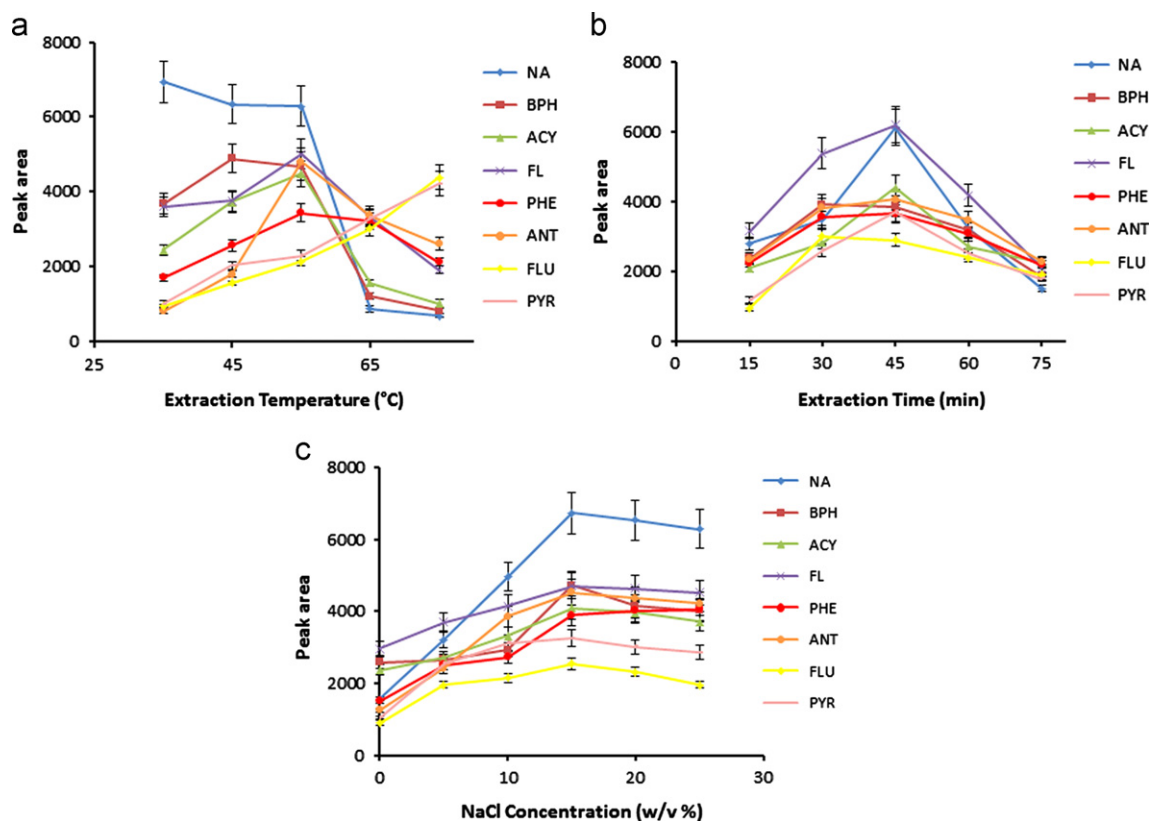


Fig. 5. Effect of extraction parameters on the extraction efficiency: (a) extraction temperature, (b) extraction time and (c) NaCl concentration; $n=3$.

LODs based on $S/N=3$ varied between 0.02 and 0.09 ng mL⁻¹. The linear ranges were determined by extracting aqueous samples with increasing concentrations. They were between 0.1 and 300 ng mL⁻¹ for the various PAHs studied. The coefficients of determination (r^2) were between 0.9802 and 0.9997. The precision of the method was determined by five replicate analyses from aqueous solutions containing 5 ng mL⁻¹ of each PAH. As Table 1 shows, the intra-day relative standard deviations (RSD%) varied between 3.2 and 7.8%, while the inter-day values were between 5.2 and 9.3%. The fiber-to-fiber reproducibilities measured by three replicate analyses from a 5 ng mL⁻¹ mixed PAH solution were between 6.2 and 11.3%.

In Table 2, the validation parameters have been compared with the values reported by other research groups [15–17,22,33].

It is seen that the results for the present method are comparable or better than ones reported elsewhere.

3.5. Real samples

To evaluate the efficiency of the proposed method, it was applied to several real samples including, a wastewater sample from Zarand Coal Processing Industries (Zarand, Iran), a well water sample collected from the vicinity of the above industry and a tap water sample collected from the Shahid Bahonar University Campus (SBUC). Three replicate analyses were performed on each sample, and compound identification was confirmed using GC/MS. The results are depicted in Table 3.

Table 1

Limit of detection (LOD) at ng mL⁻¹, percent recovery, linear range (LR) at ng mL⁻¹, coefficient of determination (r^2) and RSD (%).

Compound	LOD	Recovery (%) ^a	LR	r^2	RSD (%) ^a		
					Intra-day (N=5)	Inter-day (N=5)	Fiber-to-fiber (N=3)
Naphthalene	0.08	112	0.5–100	0.9903	5.4	8.9	10.2
Biphenyl	0.04	88	0.5–100	0.9971	6.6	7.6	8.9
Acenaphthylene	0.05	102	0.5–100	0.9997	3.2	5.2	6.2
Fluorene	0.02	96	0.1–100	0.9981	6.2	9.3	8.1
Phenanthrene	0.04	94	0.1–300	0.9957	4.8	7.5	6.8
Anthracene	0.03	81	0.1–300	0.9802	7.8	9.2	11.3
Fluoranthene	0.07	97	0.5–300	0.9919	4.5	6.1	5.9
Pyrene	0.09	94	0.5–300	0.9913	5.7	7.8	9.8

^a Measure in 5 (ng mL⁻¹) concentration.

Table 2

Comparison of linear ranges (LR), limits of detection (LOD), and relative standard deviations (RSD%) of the present SPME-GC with other works. All the concentrations are at ng mL⁻¹ and indicated in parenthesis.

Compound	Reference					
	Present work MWCNTs/PoPD/GC-FID	[15] PDMS/DVB/GC-MS	[16] PIL ^a /GC-MS	[17] MWCNTs/GC-FID	[22] PPY/DS/GC-MS	[33] PDMS/DVB/GC-FID
Naphthalene	0.5–100 ^b	0.2–60	0.5–20	0.1–100	0.5–100	0.5–100
	0.08 ^c	0.07	0.1	0.06	0.16	0.1
	5.4 ^d (5)	11.2	12 (5)	6.7 (10)	6.8 (2)	7 (10)
Biphenyl	0.5–100	-	-	0.1–100	-	-
	0.04	-	-	0.07	-	-
	6.6 (5)	-	-	5.4 (10)	-	-
Acenaphthylene	0.5–100	0.1–60	0.5–20	0.1–100	0.5–100	0.5–100
	0.05	0.03	0.06	0.05	0.09	0.1
	3.2 (5)	6.9	13 (5)	5.7 (10)	3.5 (2)	9 (10)
Fluorene	0.1–100	0.01–60	0.5–20	0.1–100	0.5–100	0.5–100
	0.02	0.005	0.05	0.04	0.05	0.08
	6.2 (5)	16.7	9.2 (5)	4.1 (10)	2.6 (2)	6 (10)
Phenanthrene	0.1–300	0.1–60	0.5–20	0.1–100	0.5–100	0.1–20
	0.04	0.04	0.25	0.03	0.06	0.04
	4.8 (5)	4.9	13 (5)	8.5 (10)	5.3 (2)	8 (10)
Anthracene	0.1–300	0.05–60	0.5–20	-	-	0.1–20
	0.03	0.02	0.1	-	-	0.03
	7.8 (5)	2.0	9.4 (5)	-	-	9 (10)
Fluoranthene	0.5–300	0.1–60	0.5–20	0.5–50	0.5–100	0.1–20
	0.07	0.03	0.08	0.07	0.12	0.03
	4.5 (5)	6.6	9.3 (5)	7.8 (10)	4.8 (2)	8 (10)
Pyrene	0.5–300	0.1–60	0.5–20	-	1–100	0.1–20
	0.09	0.03	0.09	-	0.13	0.03
	5.7 (5)	4.9	13 (5)	-	6.9 (2)	6 (10)

^a Polymeric ionic liquid.

^b The first row of figures for each compound indicates linear range (ngmL⁻¹)

^c The second row of figures for each compound indicates detection limit (ngmL⁻¹)

^d The last row of figures for each compound indicates RSD (%)

Table 3
Results obtained for real samples.

Compound	Concentration (ng mL ⁻¹)		
	Wastewater	Well water	Tap water
Naphthalene	ND	ND	ND
Biphenyl	ND	ND	ND
Acenaphthylene	ND	ND	ND
Fluorene	ND	2.5 (± 0.03)	ND
Phenanthrene	4.5 (± 0.05) ^a	3.3 (± 0.04)	ND
Anthracene	5.2 (± 0.07)	ND	ND
Fluoranthene	4.8 (± 0.04)	3.2 (± 0.03)	ND
Pyrene	5.3 (± 0.06)	2.2 (± 0.03)	ND

ND means not detected.

^a Each figure indicates SD.

The analyte percent recovery of the method was evaluated by spiking a sample of SBUC water sample at 5 ng mL⁻¹ of each PAH. The recoveries were between 81 and 112% (Table 1).

4. Conclusion

This work shows that MWCNTs/PoPD nanocomposite, which is electrochemically polymerized on the surface of stainless steel wire, can be used as an efficient HS-SPME fiber for the extraction of PAHs from aqueous samples. The proposed coating has a porous surface structure with high extraction capacity. The lifetime of the coating was such that a single fiber could be used at least 90 times for the HS-SPME analysis of PAHs. The fiber was thermally stable at temperature up to 300 °C. The combination of HS-SPME by MWCNTs/PoPD fiber with GC/FID offers significant analytical performance, very good sensitivity and reasonable precision. Various real samples were chosen to evaluate the reliability of this method which revealed high recoveries for the PAHs studied. It seems that this composite coating has a considerable potential for preconcentration and determination of other analytes as well.

References

- [1] M. Mumtaz, J. George, Toxicological profile for polycyclic aromatic hydrocarbons, U.S. Department of Health and Human Services, Agency for Toxic Substances and Disease Registry, Atlanta, GA, USA, 1995.
- [2] J. Li, X. Shang, Z. Zhao, R.L. Tanguay, Q. Dong, C. Huang, J. Hazard. Mater. 173 (2010) 75–81.
- [3] A.I. Barrado-Olmedo, R.M. Perez-Pastor, S. Garcia-Alonso, Talanta 101 (2012) 428–434.
- [4] A. Ishizaki, K. Saito, N. Hanioka, S. Narimatsu, H. Kataoka, J. Chromatogr. A 1217 (2010) 5555–5563.
- [5] A. Ramesh, S.A. Walker, D.B. Hood, M.D. Guillen, K. Schneider, E.H. Weyand, J. Toxicol. 23 (2004) 301–333.
- [6] K.B. Okona-Mensah, J. Battershill, A. Boobis, R. Fielder, Food Chem. Toxicol. 43 (2005) 1103–1116.
- [7] W. Xue, D. Warshawsky, Toxicol. Appl. Pharmacol. 206 (2005) 73–93.
- [8] D.H. Phillips, Mutat. Res. 443 (1999) 139–147.
- [9] S. Dasgupta, K. Banerjee, S. Utture, P. Kusari, S. Wagh, K. Dhimal, S. Kolekar, P.G. Adsule, J. Chromatogr. A 1218 (2011) 6780–6791.
- [10] X. Song, J. Li, S. Xu, R. Ying, J. Ma, C. Liao, D. Liu, J. Yu, L. Chen, Talanta 99 (2012) 75–82.
- [11] F. Alarcon, M.E. Baez, M. Bravo, P. Richter, E. Fuentes, Talanta 100 (2012) 439–446.
- [12] M.S. Garcia-Falcon, B. Cancho-Grande, J. Simal-Gandara, Water Res. 38 (2004) 1679–1684.
- [13] Z. Qin, L. Bragg, G. Ouyang, J. Pawliszyn, J. Chromatogr. A 1196 (2008) 89–95.
- [14] J.F. Liu, N. Li, G.B. Jiang, J.M. Liu, J.A. Jonsson, M.J. Wen, J. Chromatogr. A 1066 (2005) 27–32.
- [15] N. Aguinaga, N. Campillo, P. Vinas, M.H. Cordoba, Anal. Chim. Acta 596 (2007) 285–290.
- [16] L. Pang, J.F. Liu, J. Chromatogr. A 1230 (2012) 8–14.
- [17] Sh. Maghsoudi, E. Noroozian, Chromatographia 75 (2012) 913–921.
- [18] N. Ratola, A. Alves, N. Kalogerakis, E. Psillakis, Anal. Chim. Acta 618 (2008) 70–78.
- [19] A. Mollahosseini, E. Noroozian, Anal. Chim. Acta 638 (2009) 169–174.
- [20] H. Asadollahzadeh, E. Noroozian, Sh. Maghsoudi, Anal. Chim. Acta 669 (2010) 32–38.
- [21] J. Pawliszyn, Solid-Phase Microextraction: Theory and Practice, Wiley-VCH Inc., New York, 1997.
- [22] A. Mohammadi, Y. Yamini, N. Alizadeh, J. Chromatogr. A 1063 (2005) 1–8.
- [23] F. Cataldo, Eur. Polym. J. 32 (1996) 43–50.
- [24] Y.Q. Dai, D.M. Zhou, K.K. Shiu, Electrochim. Acta 52 (2006) 297–303.
- [25] C. Malitesta, F. Palmisano, L. Torsi, P.G. Zamboni, Anal. Chem. 62 (1990) 2735–2740.
- [26] S.R. Sivakumar, R. Saraswathi, J. Appl. Electrochem. 34 (2004) 1147–1152.
- [27] S. Myler, S. Eaton, S.P.J. Higson, Anal. Chim. Acta 357 (1997) 55–61.
- [28] S. Iijima, Nature 354 (1991) 56–58.
- [29] C.M. Niu, E.K. Sichel, R. Hoch, D. Moy, H. Tennet, Appl. Phys. Lett. 70 (1997) 1480–1482.
- [30] H.D. Wagner, O. Lourie, Y. Feldman, R. Tenne, Appl. Phys. Lett. 72 (1998) 188–190.
- [31] D. Qian, E.C. Dickey, R. Andrews, T. Rantell, Appl. Phys. Lett. 76 (2000) 2868–2870.
- [32] D. Hu, C. Peng, G.Z. Chen, ACS Nano 4 (2010) 4274–4282.
- [33] M.C. Wei, J.F. Jen, Talanta 72 (2007) 1269–1274.